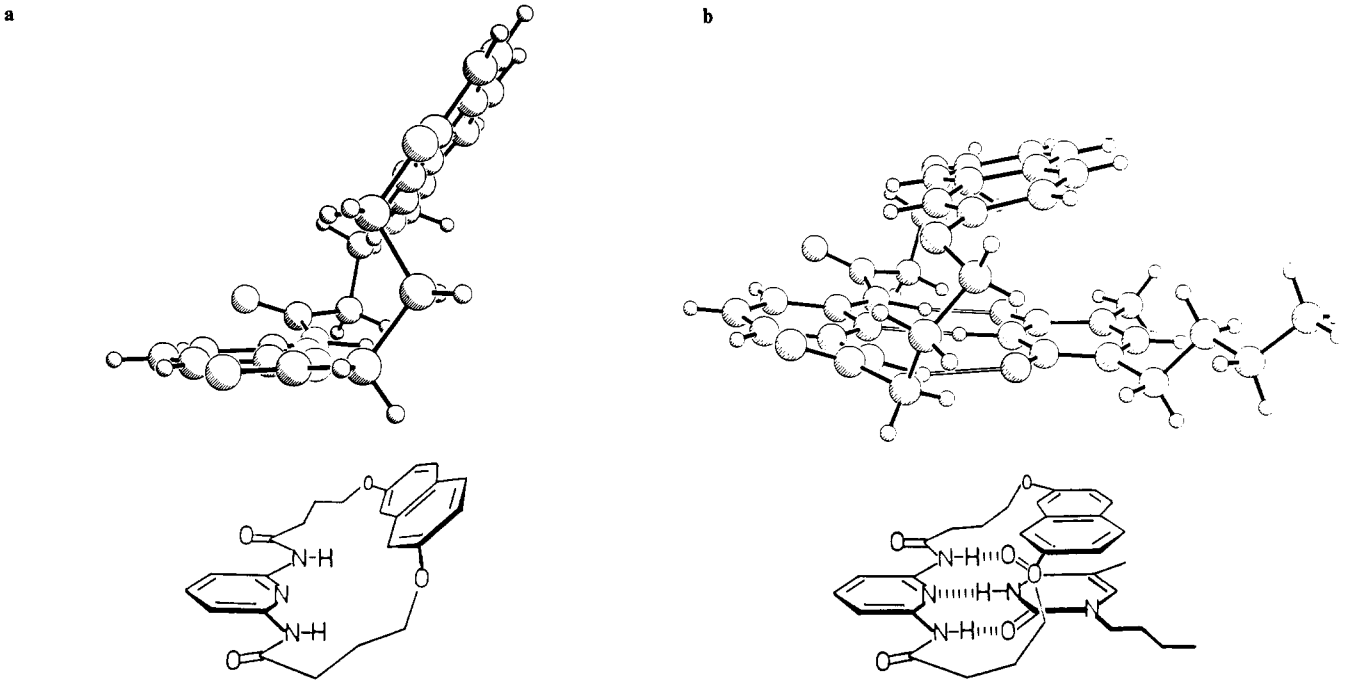

Figure 1. (a) X-ray structure of **1** and (b) X-ray structure of the complex between **1** and **5**.

downfield by 2.25 and 2.6 ppm, respectively, reflecting the formation of a triple hydrogen-bonded complex.[15] However, upfield shifts (of approximately 0.3 ppm) are seen in the thymine-6-proton, -ring methyl, and -*N*-methylene resonances while no significant shift is found for the alkyl methyl group. The selective upfield shifts of certain substrate protons are consistent with the close approach of the naphthalene to the substrate and its participation in binding.[16,17] These results are in contrast to those with 2,6-dibutyramidopyridine[15] which shows downfield shifts of its NH protons on hydrogen bonding to **5** but exhibits no upfield shifts in the substrate protons.

The structure of the complex **1**:**5** was confirmed by X-ray crystallography (Figure 1b).[18] Three hydrogen bonds are formed between the pyridine and thymine rings with distances of (N···N) 3.06, (N···O) 2.87, and 2.99 Å which are comparable to those in related complexes.[15] The naphthalene now lies approximately parallel (14°) to the plane of the thymine substrate at a closest inter-plane contact of 3.37 Å. The position of the naphthalene directly above the substrate accounts for the upfield shift of those protons on the periphery of the thymine and the absence of a shift on those protons distant from the naphthalene ring current. The angle between the pyridine and naphthalene planes is now 161.6°. Thus, on substrate complexation, **1** acts like a "molecular hinge" and swings the naphthalene unit through a 34.1° arc to within van der Waals distance of the thymine ring. This induced fit behavior in a synthetic molecule directly mimics the recognition of nucleotides by ribonuclease T_1 in which a tyrosine residue moves into place above the bound guanine.[2]

In summary, we have developed a new class of biomimetic receptors for nucleotide base substrates that employs the recognition strategy of substrate-induced organization of the binding site (induced fit). We are currently extending this approach to the other important nucleotide bases as well as to hydrogen-bonded nucleotide base pairs.

Acknowledgment. We thank the National Institutes of Health for partial support (GM-35208) of this work and Bart Kahr for his assistance with the X-ray analyses.

Supplementary Material Available: Crystallographic details for **1** and **1**:**5** including tables of atomic coordinates, thermal parameters, bond angles, and bond lengths (22 pages). Ordering information is given on any current masthead page.

(15) Feibush, B.; Figueroa, A.; Charles, R.; Onan, K. D.; Feibush, P.; Kargar, B. L. *J. Am. Chem. Soc.* **1986**, *108*, 3310.

(16) This two-point binding is confirmed by the association constants (K_a) which show an increase from 90 M^{-1} for simple 2,6-dibutyramidopyridine[15] to 290 M^{-1} for **1**. K_a measurements were made by monitoring the chemical shifts of the amide protons as a function of 1-butylthymine concentration and analyzing the data by the Foster-Fife modification of the Scatchard plot. Foster, R.; Fife, C. A. *Prog. Nucl. Magn. Reson. Spectrosc.* **1969**, *4*, 1.

(17) For other molecular complexes involving induced aromatic stacking interactions, see: Colquhoun, H. M.; Goodings, E. P.; Maud, J. M.; Stoddart, J. F.; Williams, D. J.; Wolstenholme, J. B. *J. Chem. Soc., Chem. Commun.* **1983**, 1140 and references therein.

(18) Crystals grown by slow evaporation of a 1:1 mixture of **1** and **5** in methylene chloride–heptane.

Far-Ultraviolet Resonance Raman Scattering: Highly Excited Torsional Levels of Ethylene

Roseanne J. Sension, Leland Mayne, and Bruce Hudson*

Department of Chemistry & Chemical Physics Institute
University of Oregon, Eugene, Oregon 97403
Received April 15, 1987

Ultraviolet resonance Raman scattering[1-3] has proven to be a powerful technique for the determination of electronic state symmetry,[4-6] vibronic coupling,[7] geometry changes,[8-10] and dissociation dynamics[11,12] of excited electronic states. These Raman spectra often exhibit transitions to highly excited vibrational levels,[2,8] providing new information about the ground electronic state. In a previous study,[10] the Raman spectrum of ethylene was

(1) Hudson, B. *Spectroscopy* **1986**, *1*, 22-31.
(2) Hudson, B.; Kelly, P. B.; Ziegler, L. D.; Desiderio, R. A.; Gerrity, D. P.; Hess, W.; Bates, R. In *Advances in Laser Spectroscopy*; Garetz, B. A., Lombardi, J. R., Eds.; John Wiley & Sons: New York, 1986; Vol. 3, pp 1-32.
(3) Hudson, B. In *Time-Resolved Vibrational Spectroscopy*; Laubereau, A.; Stockburger, M., Eds.; Springer-Verlag: Berlin, 1985; pp 170-174.
(4) Gerrity, D. P.; Ziegler, L. D.; Kelly, P. B.; Desiderio, R. A.; Hudson, B. *J. Chem. Phys.* **1985**, *83*, 3209-3213.
(5) Chadwick, R. R.; Gerrity, D. P.; Hudson, B. *Chem. Phys. Lett.* **1985**, *115*, 24-28.
(6) Ziegler, L. D.; Hudson, B. *J. Chem. Phys.* **1981**, *74*, 982-992.
(7) Ziegler, L. D.; Hudson, B. *J. Chem. Phys.* **1983**, *79*, 1134-1137.
(8) Desiderio, R. A.; Gerrity, D. P.; Hudson, B. *Chem. Phys. Lett.* **1985**, *115*, 29-33.
(9) Ziegler, L. D.; Hudson, B. *J. Phys. Chem.* **1984**, *88*, 1110-1116.
(10) Ziegler, L. D.; Hudson, B. *J. Chem. Phys.* **1983**, *79*, 1197-1202.
(11) Ziegler, L. D.; Kelly, P. B.; Hudson, B. *J. Chem. Phys.* **1984**, *81*, 6399-6400.
(12) Ziegler, L. D. *J. Chem. Phys.* **1986**, *84*, 6013-6026.

0002-7863/87/1509-5036$01.50/0

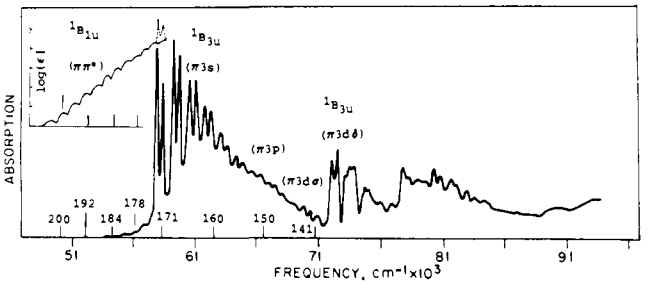

Figure 1. The absorption spectrum of ethylene in the 50 000–95 000-cm^{-1} region (from 18). The inset shows the low energy N → V transition region on a logarithmic scale (from Merer and Mulliken, ref 13). The excited state assignments[14,17] and the frequencies used for Raman excitation are indicated by the corresponding wavelength in nm.

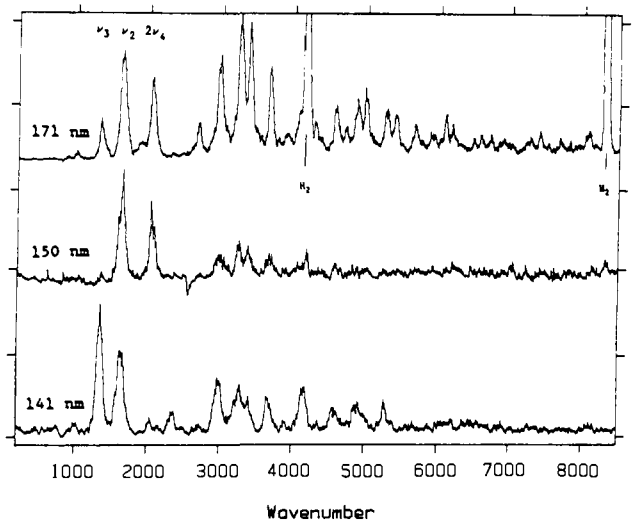

Figure 2. Resonance Raman spectra of ethylene obtained with 171-, 150-, and 141-nm radiation. Some of the major vibrational bands are indicated. The bands at multiples of 4155 cm^{-1}, labeled "H_2", are spurious stimulated Raman shifted lines from the hydrogen Raman shifting cell. These are used in the frequency calibration procedure. The sample was a stream of ethylene in a nitrogen atmosphere. The region near 2000 cm^{-1} of the 141-nm spectrum is obscured by absorption due to the first Lyman–Birge–Hopfield band of nitrogen. This includes the region of the $2\nu_4$ band.

determined with excitation at 266, 213, and 193 nm. Strong activity was observed in the C=C stretch (ν_2), the HCH scissors mode (ν_3), and, of greatest interest, transitions involving 2 and 4 quanta of the a_u torsional mode, ν_4, confirming the expectation[13,14] that ethylene is twisted in its low lying excited states.

We have extended the technique of far ultraviolet resonance Raman spectroscopy to wavelengths as short as 141.2 nm and have applied this method to a further study of ethylene. Spectra have been obtained with use of radiation at 192, 184, 178, 171, 160, 150, and 141 nm resulting from stimulated Raman shifting in hydrogen gas by using 532- or 266-mm input generated by a powerful Nd:YAG laser.[15] The Raman spectra obtained exhibit many highly excited vibrational levels. Of greatest interest is the

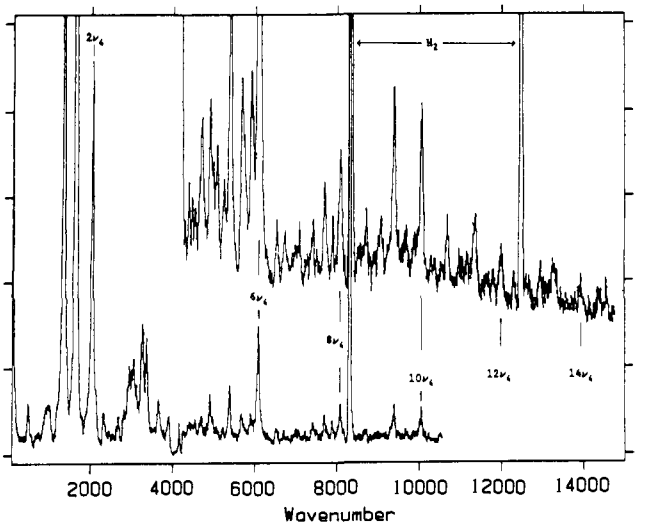

Figure 3. The resonance Raman spectrum of ethylene obtained with 184-nm radiation. The upper trace is an independent scan at higher resolution and sensitivity. The bands assigned as even quanta of ν_4 are indicated. The $4\nu_4$ band is quite close to the first Stoke's shifted hydrogen line at 4155 cm^{-1}. The frequency of the $4\nu_4$ transition is known from previous work.[10] In the lower scan shown here, this region has been strongly reduced in intensity by narrowing the slit.

series of even overtones of the torsional mode with up to 14 quanta of excitation.

The absorption spectrum of ethylene is shown in Figure 1. The laser lines that have been used for Raman excitation are indicated as are the assignments of the absorption bands.[14,17] It is clear that several distinct excited states are probed with the radiation used. The resulting Raman spectra (Figure 2) are dominated by bands corresponding to transitions involving the HCH mode ν_3, the C=C stretch, ν_2, and even quanta of ν_4 and combinations and overtones of these bands. There are many other vibrations. The spectra obtained at different excitation wavelengths exhibit large variations in relative band intensity reflecting differences in the geometry of the excited states making the major contribution to the Raman process at that wavelength. One example of this variation in intensity is the large increase in the ν_3 band relative to ν_2 in the 141-nm spectrum compared to that observed at 150 or 171 nm. Excitation at 141 nm is near resonance with the first strong band of the transition assigned as the $^1B_{3u}$ $\pi 3d\delta$ Rydberg transition.[14,17] The large intensity of the ν_3 band is consistent with the assignment of significant activity of ν'_3 in this transition.[14,17]

The spectra obtained with 184- and 178-nm radiation, resonant with the N → V $\pi\pi^*$ transition, exhibit many lines including a long progression in even quanta of the C=C torsional mode ν_4 (Figure 3). The bands assigned to this progression are at 2046, 4076, 6087, 8080, 10062, 11997, and 13937 cm^{-1}. The accuracy of these values with present calibration methods is about 10 cm^{-1}. A simple one-dimensional treatment of the internal rotation problem using a fixed moment of inertia and a potential of the form $V(\phi) = (V_o/2)[1 - \epsilon - \cos(2\phi) + \epsilon\cos(4\phi)]$ with V_o = 33400 cm^{-1} and ϵ = 0.047 results in calculated even overtones at 2046, 4076, 6089, 8082, 10051, 11996, and 13912 cm^{-1}. These are in good agreement with the observed values considering the simplicity of this model. This agreement confirms the assignments and establishes the torsional barrier height as near 33400 cm^{-1}. A cos (2ϕ) potential (ϵ = 0) is considerably too "anharmonic"; a value of V_o of 27600 cm^{-1} with this functional form results in calculated levels of 2044, 4047, 6009, 7928, 9802, 11629, and 13407 cm^{-1}, systematically low for the higher levels by as much as 500 cm^{-1}.

(13) Merer, A. J.; Mulliken, R. S. *Chem. Rev.* **1969**, *69*, 639–656. Merer, A. J.; Mulliken, R. S. *J. Chem. Phys.* **1969**, *50*, 1026–1027. Foo, P. D.; Innes, K. K. *J. Chem. Phys.* **1974**, *60*, 4582–4589.

(14) Robin, M. B. *Higher Excited States of Polyatomic Molecules*; Academic Press: New York, 1975; Vol. II, pp 2–22; 1985; Vol. III, pp 213–227.

(15) The experimental arrangement is similar to that previously described[1,2,16] modified for wavelengths shorter than the absorption cutoff of air by use of a containment box purged with nitrogen and CaF_2 and MgF_2 windows, lenses, and photomultiplier window. Reflective collection optics are used. Excitation is through a hole in a spherical mirror so that the Raman scattered radiation is observed in back scattering. A partial description of this apparatus is given in the following: Kelly, P. B.; Ruggiero, A.; Li, S.; Harhay, G.; Strahan, G. D.; Hudson, B. In *Tenth International Conference on Raman Spectroscopy*; Peticolas, W. L.; Hudson, B., Eds.; University of Oregon: Eugene, OR, 1986; p 20.11–20.12.

(16) Hudson, B.; Mayne, L. C. In *Biological Applications of Raman Spectroscopy*; Spiro, T. G., Ed.; John Wiley: New York, 1987; pp 181–200.

(17) McDiarmid, R. *J. Phys. Chem.* **1980**, *84*, 64–70.

(18) Geiger, J.; Wittmaack, K. *Z. Naturforsch., A: Astrophys., Phys., Phys. Chem.* **1965**, *20A*, 628–629.

These spectra demonstrate the feasibility of ultraviolet resonance Raman spectroscopy in the far ultraviolet region with use of existing commercial laser sources. They also demonstrate the utility of this technique for observation of highly excited vibrational levels of a small yet interesting molecule.

Acknowledgment. This research is supported by NSF Grant CHE-85-11799. We thank Suzanne Hudson for writing the program for the determination of the energy levels of the internal rotation potential used in this work. We also acknowledge Shijian Li and Peter Kelly for the construction of the far UV Raman spectrometer.

Carbon-13 CIDNP Investigation of the Thermal Decomposition of *tert*-Butyl Phenylperacetate[1]

John Kurhanewicz and George R. Jurch, Jr.*

Department of Chemistry, University of South Florida Tampa, Florida 33620

Received February 6, 1987

The initial work of Bartlett and Hiatt[2] led the authors to postulate two mechanisms for the thermal decomposition of *tert*-butyl peresters, R-C(O)-O-O$(CH_3)_3$: a one bond O–O cleavage (nonconcerted) when R was not a stable alkyl radical and a concerted O–O and R–C bond cleavage when R was a stable radical. Subsequent kinetic work involving: substituent effects,[3] cage effects,[4] stereochemical effects,[5] secondary deuterium isotope effects,[6] and activation volumes,[7] viscosity dependence,[8] ring strain effects,[9] and isotopic labeling[10] raised some serious questions about the twofold nature of the thermal decomposition but even revised versions still contained the two pathways. An initial proton CIDNP investigation of the thermal decomposition of *tert*-butyl phenylperacetate (I) indicated a number of net polarizations which arose from sorting encounters between triplet radical pairs[11] and agreed with earlier unpublished proton CIDNP results obtained for *tert*-butyl perpivalate.[12]

In this work we will describe carbon-13 polarizations obtained during the thermal decomposition of labeled (I)[13] in hexachloroacetone and cyclohexanone.[14] The polarizations are listed in Table I. All polarizations were assigned based on the addition of known compounds to the decomposed sample and GC-mass spectral analysis of the decomposed sample.[15] Individual carbon assignments were aided by multiplicity determinations by using NOE, SEFT, or INEPT II multiplicity analysis.

Table I. CIDNP Polarizations during the Thermal Decomposition of Labeled[a] *tert*-Butyl Phenylperacetate in Hexachloroacetone and Cyclohexanone

compd	carbon[b]	chem shift (ppm)	polarztn obsd	net equation μ	ϵ	Δ_g	a_i
Polarizations in Hexachloroacetone							
bibenzyl	C-2	141.8	E	+	−	−	−
cis-stilbene	C-1	124.4	A	+	−	−	+
	C-2	131.5	E	+	−	−	−
benzyl phenyl acetate	carbonyl	170.2	E	+	+	+	−
carbon dioxide		124.2	E	+	+	+	−
benzyl chloride	C-1	45.6	A	+	−	−	+
	C-2	137.5	E	+	−	−	−
	C-3	128.3	A	+	−	−	+
hexachloroethane		107.1	E	+	−	+	+
1,1-dichlorostyrene	C-1	121.3	A	+	+	+	+
	C-2	128.0	E	+	+	−	+
	C-3	135.2	A	+	+	−	−
benzyl	carbonyl	180.4	E	+	+	+	−
pentachloroacetone	CCl	83.4	A	+	+	+	+
	C-1	51.9	E	+	+	−	+
	C-2	135.2	A	+	+	−	−
Polarizations in Cyclohexanone							
benzyl *tert*-butyl ether	C-2	140.61	A	+	+	−	−
	C-3	128.80	E	+	+	−	+
bibenzyl	C-1	37.22	A	+	−	−	+
	C-2	141.76	E	+	−	−	−
	C-3	128.41	A	+	−	−	+
benzyl phenyl acetate	carbonyl	171.60	E	+	+	+	−
carbon dioxide		124.31	E	+	+	+	−
toluene	C-1	20.56	E	+	−	+	+
	C-2	138.12	A	+	−	+	−
α-benzylcyclohexanone	carbonyl	209.19	E	+	+	+	−
	C-α	51.89	A	+	+	+	+
	C-1	33.52	E	+	+	−	+
	C-2	144.51	A	+	+	−	−

[a] Carbon-13 labeled carbonyl. [b] Compounds are numbered in the following way

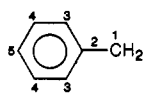

By using the qualitative CIDNP rules of Kaptein[16] and the experimental net polarizations, the signs of the product factor, ϵ, and multiplicity, μ, were deduced by examining all the possible reaction pathways. These results are presented in Table I and indicate all the steps leading to polarization involve triplet radical pairs. This can be explained by a phenomenon initially coined "radical pair substitution", by den Hollander and Kaptein.[17,18]

A mechanism that can account for all the CIDNP and kinetic data is shown in Scheme I. The proposed mechanism involves nonconcerted cleavage to form a singlet *tert*-butyloxy–phenylacetyloxy radical pair. Spin correlation is lost due to the *tert*-butoxy radical, as indicated by the earlier proton CIDNP stud-

(1) Presented at the 192nd National Meeting of the American Chemical Society, Anaheim, CA, Sept. 11, 1986; paper 265.
(2) Bartlett, P. D.; Hiatt, R. R. *J. Am. Chem. Soc.* **1958**, *80*, 1398.
(3) (a) Bartlett, P. D.; Ruchardt, C. *J. Am. Chem. Soc.* **1960**, *82*, 1756. (b) Ruchardt, C.; Bock, H. *Chem. Ber.* **1964**, *100*, 654.
(4) (a) Lorand, J. P. *J. Am. Chem. Soc.* **1974**, *96*, 2867.
(5) (a) Engstrom, J. P.; Greene, F. D. *J. Org. Chem.* **1972**, *37*, 968. (b) Koeing, T.; Owens, J. M. *J. Am. Chem. Soc.* **1973**, *95*, 8484.
(6) (a) Koenig, T.; Wolf, R. *J. Am. Chem. Soc.* **1969**, *91*, 2574. (b) Koenig, T.; Huntington, J.; Cruthoff, R. *J. Am. Chem. Soc.* **1970**, *92*, 5413.
(7) (a) Neuman, R. C., Jr. *Acc. Chem. Res.* **1972**, *5*, 381. (b) Neuman, R. C., Jr.; Pankratz, R. P. *J. Am. Chem. Soc.* **1973**, *95*, 8372.
(8) Pryor, W. A.; Smith, K. *J. Am. Chem. Soc.* **1970**, *92*, 5403.
(9) (a) Ruchardt, C. *Angew. Chem. Int. Ed. Engl.* **1970**, *9*, 830 and literature cited therein. (b) For a review, see: Ruchardt, C. *Fortschr. Chem. Forsch.* **1966**, *6*, 251. (c) Lorand, J. P.; Chodroff, S. D.; Wallace, R. W. *J. Am. Chem. Soc.* **1968**, *90*, 5266.
(10) Goldstein, M. J.; Judson, H. A. *J. Am. Chem. Soc.* **1970**, *92*, 4120.
(11) Spence, J. R.; Jurch, G. R., Jr. Southeast Regional ACS Meeting, Charleston, SC, Nov. 7, 1973.
(12) Kaptein, R. In *Chemically Induced Dynamic Nuclear Polarization*; Lepley, A. R., Closs, G. L., Eds.; Wiley-Interscience: 1973; p 137, unpublished results.
(13) This perester was prepared by the reaction of C-13 carbonyl labeled phenylacetic acid with thionyl chloride and then the subsequent reaction of the acid chloride with *tert*-butyl hydroperoxide according to the procedure of Bartlett and Hiatt:[2] IR (neat) 3075–3025 (aromatic C–H), 2956–2988 (aliphatic C–H), 1776 (carbonyl), 1605–1450 (aromatic C=C), 1195 (C–O), 850 (O–O), 705 (5 adjacent hydrogens) cm^{-1}; ^1H NMR ($CDCl_3$) 1.23 (s, 9 H), 3.58 (s, 2 H), 7.26 (s, 5 H) ppm; ^{13}C NMR ($CDCl_3$) 25.74 (q, 3 C), 38.26 (t, 1 C), 83.28 (s, 1 C), 127.10 (d, 1 C), 128.40 (d, 2 C), 128.89 (d, 2 C), 132.68 (s, 1 C), 168.33 (s, 1 C) ppm.
(14) Labeled *tert*-butyl phenylperacetate was decomposed inside the probe of a Joel FX90Q at temperatures ranging from 70 to 135 °C by using deuteriated Me_2SO as a lock.
(15) The GC–MS product studies were carried out on a Hewlett Packard 5890A GC with a 59700 series mass selective detector by using a 2 M capillary carbowax column with a 0.20 mm diameter (HP 298-12-09-B). The product mixture was diluted (100/1) with methanol and the GC run temperature programmed from 70 to 240 °C.
(16) Kaptein, R. *J. Chem. Soc.* D **1971**, 732. The net equation consists of four terms ($T_N = \mu\epsilon\Delta g a_i$); μ refers to the multiplicity of the radical pair at the time of its formation, ϵ is evaluated from the type of product-forming reaction, Δg is the difference in spectroscopic splitting factors of the radical pair, and a_i is the sign of the hyperfine coupling constant.
(17) den Hollander, J. A.; Kaptein, R. *Chem. Phys. Lett.* **1976**, *41*, 257.
(18) Kaptein, R. *J. Am. Chem. Soc.* **1972**, *94*, 6251.

0002-7863/87/1509-5038$01.50/0